Nanoscale

Accepted Manuscript

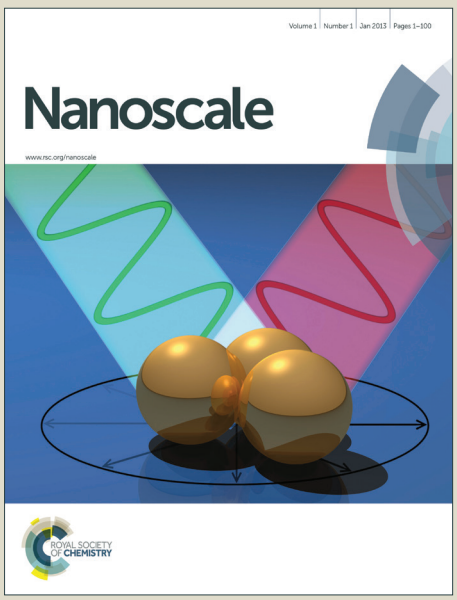

ROYAL SOCIETY OF CHEMISTRY

www.rsc.org/nanoscale

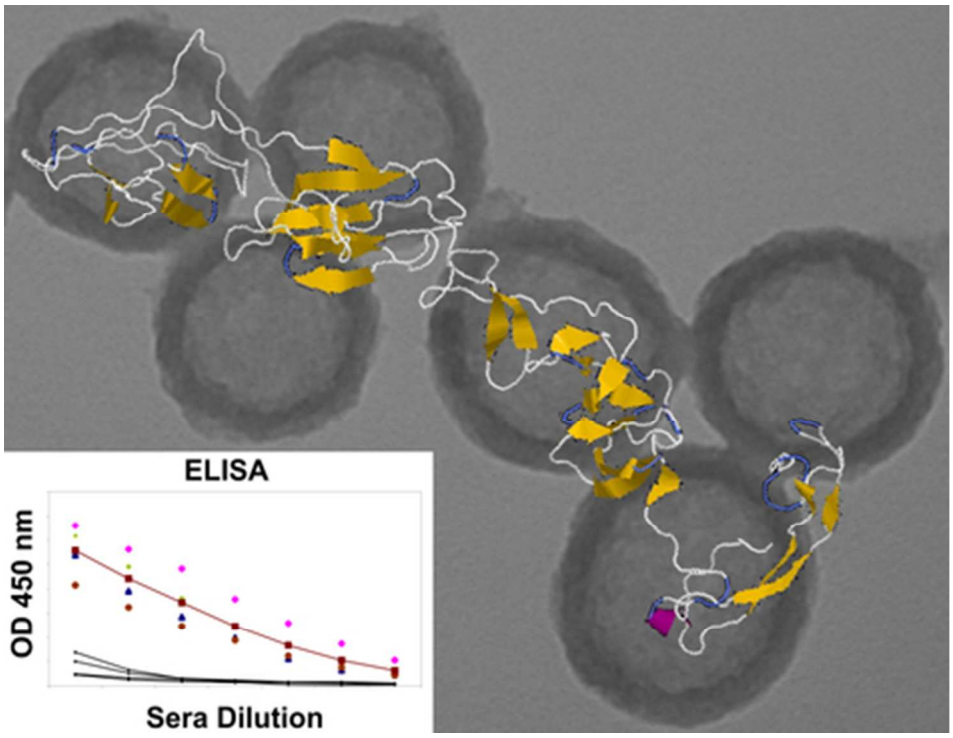

Immunisation studies in mice show that hollow mesoporous silica nanoparticles act as both a delivery vehicle and adjuvant for the viral protein E2 from Bovine Viral Diahorrea Virus.
39x30mm (300 x 300 DPI)

Nanoscale

RSCPublishing

ARTICLE

In vivo delivery of Bovine Viral Diahorrea Virus, E2 protein using Hollow Mesoporous Silica Nanoparticles.

Cite this: DOI: 10.1039/x0xx00000x

Received 00th January 2012,
Accepted 00th January 2012

DOI: 10.1039/x0xx00000x

www.rsc.org/

D. Mahony[a], A. S. Cavallaro[a]†, K. T. Mody[a]†, L Xiong[b], T. J. Mahony[a], S. Z. Qiao[b] and N. Mitter[a]

Our work focuses on the application of mesoporous silica nanoparticles as a combined delivery vehicle and adjuvant for vaccine applications. Here we present results using the viral protein, E2, from Bovine Viral Diarrhoea Virus (BVDV). BVDV infection occurs in the target species of cattle and sheep herds worldwide and is therefore of economic importance. E2 is a major immunogenic determinant of BVDV and is an ideal candidate for the development of a subunit based nanovaccine using mesoporous silica nanoparticles. Hollow type mesoporous silica nanoparticles with surface amino functionalisation (termed HMSA) were characterised and assessed for adsorption and desorption of E2. A codon-optimised version of the E2 protein (termed Opti-E2) was produced in *Escherichia coli*. HMSA (120 nm) had an adsorption capacity of 80 µg Opti-E2/mg HMSA and once bound E2 did not dissociate from the HMSA. Immunisation studies in mice with a 20 µg dose of E2 adsorbed to 250 µg HMSA was compared to immunisation with Opti-E2 (50 µg) together with the traditional adjuvant *Quillaja saponira* Molina tree saponins (QuilA, 10 µg). The humoral responses with the Opti-E2/HMSA nanovaccine although slightly lower than those obtained for the Opti-E2+QuilA group demonstrated that HMSA particles are an effective adjuvant that stimulated E2-specific antibody responses. Importantly the cell-mediated immune responses were consistently high in all mice immunised with Opti-E2/HMSA nanovaccine formulation. Therefore we have shown the Opti-E2/HMSA nanoformulation acts as an excellent adjuvant that gives both T-helper 1 and T-helper 2 mediated responses in a small animal model. This study has provided proof-of-concept towards the development of an E2 subunit nanoparticle based vaccine.

Introduction

Bovine viral diarrhoea virus (BVDV) is a prevalent cattle infection that can cause serious mucosal lesions and other clinical manifestations such as reproductive disorders, congenital defects and persistent infections which can cause debilitating disease[1] with widespread economic impact.[2] BVDV infection can also be associated with the bovine respiratory disease complex due to the immunosuppression of infected animals.[3] An economic analysis in 2009 estimated that yearly losses of up to US$88 per animal could be attributed to infection with BVDV.[4]

BVDVs are a group of positive sense, single-stranded RNA viruses classified in the pestivirus genus within the Flaviviradae family.[5] The BVDV genome is transcribed as a single, large (~12.3 kb) open reading frame. The E2 membrane glycoprotein has been shown to be the major immunodominant protein[6] and has been the focus as a potential candidate for the development of a subunit BVDV vaccine. E2 was first cloned and expressed in a bacterial system by Yu *et al.*[7] This study showed antibodies raised against a truncated 28 KDa E2 recombinant protein were specifically able to recognise E2 from a number of BVDV strains.[7] In recent years a variety of expression systems have been used for E2 expression including: mammalian cells, [8-10] baculovirus expression,[9, 11, 12] *Rachiplusia nu per os* larvae,[13] *Drosophila melanogaster* cells.[14] Recently it has also been expressed in *Saccharomyces cerevisia,*[15] *E coli* cells[16] and in *Nicotiana tabaccum* plants.[17] The various E2 expression studies aim to produce E2 protein in sufficient quantities to allow the immunocompetence of the resulting recombinant protein to be assessed *in vivo*.

Mesoporous silica nanoparticles (MSNs) are an ideal vehicle for vaccine delivery due to their synthesis methods which allow for precise control of particle size, morphology and surface functionalisation. MSNs with an ordered pore structure and uniform pore size were first synthesised in 1992 by Mobil Corporation scientists using liquid-crystal templating and the resulting mesoporous material was designated Mobile Crystalline Materials No.41 (MCM-41). MSNs are well-tolerated in the mammalian system and this biocompatibility together with their self-adjuvant effect makes them an ideal candidate for development of a new generation of nanovaccines which can deliver recombinant protein

antigens and provide an adjuvant effect. Adjuvants act as immuno-stimulants to enhance the immune response to an antigen. Saponin based adjuvants such as Quil A and its derivatives QS21 can induce both humoral antibody and T cell-mediated immune responses.[18] Aluminium salt based adjuvants, often termed alum are widely used in veterinary vaccines and it has also been used for human vaccines.[19] Although alum induces strong humoral antibody responses it can fail to induce cell meditated immunity.[20-22] Alum can also have side effects such as formation of granulomas at the injection site when administered subcutaneously or intra-dermally.[23]
MSNs offer a useful alternative to conventional adjuvants. Various types of silica nanoparticles have been used to deliver antigens in immunisation studies that have induced both humoral and cell-mediated immune responses.[24-28]
The role of Santa Barbara Amorphous-15 (SBA-15), a silica cylinder mesostructure,as a delivery and adjuvant system was first demonstrated by Mercuri et al using a small 16.5 kDa bacterial, recombinant protein, termed *Int1ß* and *Micrurus ibiboboca* snake venom proteins in mice.[17] In this study isogenic BALB/C mice and genetically modified low and high responder mice lines were injected subcutaneously with 10 µg of *Int1ß* protein adsorbed/encapusulated in 100 µg SBA-15, 10 µg *Int1ß* protein adsorbed on alum and 10 µg *Int1*ß protein emulsified with incomplete Freund's adjuvant (IFA). The results showed that SBA-15 acted as a better adjuvant than Alum and was as effective as IFA in maintaining antibody levels during the primary response. The effectiveness of SBA-15 (1-2 µm) and silica nanoparticles termed S1 and S2 (430 and 130 nm respectively in size) as adjuvants and oral delivery vehicles have been demonstrated using bovine serum albumin (BSA) as a model antigen.[26] Mice vaccinated with BSA loaded on silica nanoparticles showed a BSA-specific immune response in the order of (S1 > S2 > SBA-15).
Hollow/rattle structured mesoporous silica nanoparticles [29] have been successfully used for the *in vitro* delivery of ibuprofen,[30] the anticancer drug doxorubicin,[31] for the delivery of a capsid protein of porcine circovirus type 2 in mice[27] and as an oral vaccine adjuvant with bovine serum albumin in mice.[26]
Currently available BVDV vaccines comprise of live attenuated or inactivated forms of the virus which may be either cytopathic or noncytopathic strains. Hence there is a need to develop a safer, cost-effective subunit based BVDV vaccine. Our approach utilises silica nanoparticles for the delivery of the E2 protein of BVDV. Nanoparticle based delivery systems for subunit vaccines can increase the presentation of the proteins to antigen presenting cells and also act as self-adjuvants to generate enhanced immune responses. The use of a nanoparticle based delivery system and strategies to increase immunogenicity for synthetic peptides as vaccines has recently been reviewed by Salvador *et al.*[32] reporting the induction of both humoral and cellular immune responses using polymeric nanoparticles and nanobeads for peptide based vaccine delivery.
In this report the hollow mesoporous silica nanoparticles surface functionalised with amino groups were used as a delivery vehicle and adjuvant towards development of a recombinant, BVDV-E2 nanovaccine. Immunisation of mice with the nanovaccine generated both antibody and cell-mediated immune responses.

RESULTS and DISCUSSION

Antibody recognition of Opti-E2 protein

One potentially limiting factor in the development of any subunit vaccine is the cost-effective, large-scale production of the antigen. A truncated version of the Opti-E2 open reading frame (ORF) was produced by PCR to remove the 3' region of the native ORF which encodes for the 93 bp membrane spanning domain.[16] The recombinant protein encoded by pET-Opti-E2 had excellent expression levels of 100-150 mg Opti-E2/l of bacterial culture.[16] This level of expression compares well to other E2 expression systems including: 30-50 mg/l in *E.coli*,[7] 10-20 mg/l of infected *Spodoptera frugiperda* cells,[11] 10 mg/l of infected *Drosophila melanogaster* cells,[14] 20 µg/gram of *Agrobacterium tumefaciens* infected tobacco leaf tissue,[33] 3.5 mg/l in mammalian HEK 293T cells and 1 µg/per infected *Rachiplasi nu* larva.[8]
To demonstrate that Opti-E2 has potential use as a subunit vaccine component, its immunogenicity was determined by Western analyses with commercially available BVDV antibodies, sera from a bovine prior to and after infection with BVDV and with mouse sera after immunisation with Opti-E2. Western hybridisation analyses showed Opti-E2 was recognised by two BVDV monoclonal antibodies (mAb-157, mAb-348), polyclonal goat, bovine anti-BVDV sera and mouse anti-E2 sera (Fig. 1). These results demonstrated that Opti-E2 is immunologically recognised and therefore useful for subunit vaccine development using HMSA particles.

Fig. 1: Western blot analysis of Opti-E2 protein with BVDV-specific antibodies. Opti-E2 protein was transferred to Hybond C membrane and visualised by ECL. Lane 1, VMRD mAb-157; lane 2, VMRD mAb-348, lane 3, VMRD Goat anti-BVDV; lane 4, bovine 554 pre BVDV-infection sera; lane 5, bovine 554 post BVDV-infection sera; lane 6, mouse sera post immunisation with E2 protein.

Characterisation of HMSA nanoparticles

The synthesised HMSA particles were of a uniform size of 120 nm (Supplementary Fig. S1) with a shell thickness of 20 nm (Fig. 2). The pore structure of HMSA was characterised by nitrogen adsorption-desorption (Fig. 3). The BET surface area and total pore volume of HMSA were 57 m^2/g and 0.35 cm^3/g, respectively. The condensation step at high relative pressure (P/P0>0.8) in the isotherm (Fig. 3A) and pore size distribution indicate HMSA possessed a high fraction of textual porosity. Fig. 4A shows the Fourier transform infrared (FTIR) spectra of HMSA. The peaks at 789 cm^{-1} and 1040 cm^{-1} (Fig. 4A) were attributed to symmetric and asymmetric stretching vibration of Si-O bond, respectively.[34] The absorption bands at 1470 cm^{-1} and those between 2850 and 3000 cm^{-1} (Fig. 4A) were assigned to the C-H bending and stretching vibrations, respectively.[31] A broad band at 1630 cm^{-1} was due to N-H bending.[3] FTIR analysis confirmed the incorporation of C18TMS and APTES into HMSA. The surface functionalisation of HMSA was further characterised by XPS spectra. The survey spectra showed the presence of Si, O, C and N elements (Fig. 4B). The high-resolution C1s XPS (Fig. 4B, left insert panel), the peaks can be assigned to two components corresponding to C-C bond at 284.6 eV and C-N bond at 286.1 eV, respectively.[35] In addition the N1s peak could be deconvoluted into two components due to amine groups (NH_2) at 399.5 eV and ammonium groups (NH_4^+) at 401.3 eV (Fig. 4B, right insert panel). These results were in agreement with published FTIR spectra.[36]

Fig. 2. The morphology and microstructure of HMSA observed by (a) SEM and (b) TEM.

Fig. 3. (a) N_2 adsorption-desorption isotherms and (b) corresponding BJH pore diameter distributions of HMSA.

Fig. 4. (A) FTIR of HMSA. (B) Survey and high-resolution C1s and N1s XPS spectra of HMSA.

In vitro compatibility of HMSA

HMSA were tested for cytotoxic effects in MDBK cells by trypan blue dye exclusion staining. Healthy, intact cells do not take up the trypan blue stain as shown by the cells alone control (Fig. 5A). Unfunctionalised Mobil Corporation Matrix-41 (MCM-41) type nanoparticles are toxic to cells and were used a positive control to induce cell death (Fig. 5B). The compromised cells were able to take up the trypan blue stain and thus showed the characteristic blue colour staining similar to the positive control (Fig. 5B). At a higher concentration of 0.1 mg/ml HMSA had a toxic effect on the MDBK cells and the compromised cells thus showed the characteristic blue colour staining (Fig. 5C). However, at a lower concentration 0.01 mg/ml, HMSA did not show cytotoxicity (Fig. 5D) and the uncompromised cells were similar in appearance to the negative control (Fig. 5A).

The cytotoxicity of silica nanoparticles depends on various factors like particle size, morphology, structure, surface properties and dosage. The *in vitro* interaction of MSNs with various cell lines including HeLa cells,[37] rodent fibroblast 3T3 cells[38] human mesenchymal stem cells[39] and human colon carcinoma [40] have been explored. Qiu *et al.*[41] highlighted that the MSNs have size and concentration-dependant cytotoxic effect on HeLa cells using 3-[4,5-dimethylthiazol-2-yl]-2,5-diphenyltetrazolium bromide assay. Duan *et al.*[42] found that the toxicity of silica nanoparticles was dosage dependant in endothelial cells as the higher concentrations of 0.1 mg/ml and 0.05 mg/ml had a significant effect on cell viability after 24 h exposure but not at the lowest dose of 0.025 mg/ml. The result from the current study shows HMSA nanoparticles were found to be toxic at a higher concentration of 0.1 mg/ml, but at the lower concentration of 0.01 mg/ml the nanoparticles were found to be non-toxic on the MDBK cell line.

Fig. 5: Cytotoxicity of nanoparticles to MDBK cells.
Trypan blue (0.2%) staining of MDBK cells after 20 hr incubation. (A) Cells only control, (B) MCM-41 0.5 mg/ml control, (C) 0.1 mg/ml HMSA and (D) 0.01 mg/ml HMSA.

Adsorption and desorption of Opti-E2

The adsorption isotherm occurs when the maximum amount of protein is adsorbed to the minimum amount of particles. Adsorption reactions for Opti-E2 were performed at 25 ^{o}C in PBS buffer (pH 7.2) which is the pH at which maximal binding will occur since the calculated isoelectric point of Opti-E2 is 7.25.[16] To determine the adsorption isotherm of Opti-E2 to HMSA, adsorption reactions were performed in which the HMSA particle concentration was kept constant and the protein concentration was varied to 300, 200, 175 and 150 µg Opti-E2 protein/mg HMSA particles then subjected to 4 hr and overnight (22 hr) incubation. The SDS-PAGE gel analyses of the adsorption supernatants and pellets showed the presence of Opti-E2 in the 4 hr and 22 hr supernatants of the reactions containing 300 and 200 µg Opti-E2 (Fig. 6). There was no Opti-E2 detected in the supernatants at 175 and 150 µg protein loading after 22 hr of incubation (Fig. 6). This indicated complete loading of the protein on HMSA at these concentrations. The unbound Opti-E2 remaining in the supernatants was quantified by protein assay. The adsorption isotherms were determined as 60 µg Opti-E2/mg HMSA after 4 hr adsorption and 80 µg Opti-E2/mg HMSA after 22 hr. For the *in vivo* immunisation studies, Opti-E2 was bound to HMSA for 22 hr.

Fig. 6: Adsorption isotherm of Opti-E2 to HMSA**.**
Adsorption reactions contained varying amounts of Opti-E2 (300, 200, 175 and 150 µg) and 2 mg HMSA. Supernatant (**S**) and particles (**P**) fractions after 4 hr (upper panel) and 22 hr (lower panel) adsorption are shown.
M: SeeBlue® Plus2 MW standard; **C**: Opti-E2 control (4 µg); **300** µg Opti-E2/2 mg HMSA S and P fractions; **200** µg Opti-E2/2mg HMSA reaction S and P fractions; **175** µg Opti-E2/2 mg HMSA reaction S and P fractions; **150** µg Opti-E2/2 mg HMSA S and P fractions.

The protein adsorption capacity of nanoparticles depends on the particle surface area, charge, pore size and the physical size of the protein antigen. Proteins with a hydrodynamic diameter which is larger than the pore diameter adsorb on the outer surface of while small proteins can enter the mesopores and therefore show higher loading.[43] This has also been found to be the case for SBA-15 with higher adsorption capacity found for the relatively small proteins cytochrome c, lysozyme and myoglobin whereas the larger proteins ovalbumin, BSA and conalbumin show lower binding capacity as they are size excluded from the internal pore surfaces.[44] Utilising the iTasser prediction software[45, 46] and the recently published E2 crystal structure, 2YQ2[47] as a structural template, Opti-E2 was hypothesised to be an elongated protein. Estimates of the physical size indicate a length of 12-13 nm and a width of 3-4 nm. Since the pore size of HMSA is 2-3 nm, the estimated size of Opti-E2 would prevent internalisation and therefore we propose that Opti-E2 adsorbs via the external surface of HMSA.

Opti-E2 protein adsorbed to HMSA nanoparticles at a capacity of 80 µg Opti-E2/mg HMSA after overnight binding. In a study using mesoporous SBA-15 particles as an adjuvant, the small 16.5 kDa bacterial recombinant protein, *Int*1ß had a binding capacity of 100 µg/mg SBA-15[24] whereas the larger BSA protein (66 kDa) bound at 40 µg/mg thiol functionalised SBA-15.

The desorption studies on Opti-E2 loaded on HMSA were performed at 37 °C to mimic the body temperature of mammals. *In vitro* desorption studies of Opti-E2 showed that once bound Opti-E2 did not dissociate from the particles (Supplementary Fig. S2). Further desorption studies using more stringent buffers showed that there was only minimal desorption of Opti-E2 in acid buffer (0.1 N HCl) and in 0.5 % SLS after 2 hr incubation and there was no additional desorption up to 24 hr (Supplementary Fig. S3A and B). A similar result was observed for BSA bound to thiol functionalised SBA-15 which showed only 2% desorption.[44] The minimal *in vitro* desorption of Opti-E2 from HMSA indicates its usefulness as a delivery vehicle with bound protein remaining intact. In fact we have shown that Opti-E2 bound HMSA remained intact for several months as evidenced by PAGE gel analysis (data not shown). Wang *et al.*[26] have demonstrated that particles with lower levels of *in vitro* desorption showed greater antibody response when used in immunisation studies. Mice vaccinated with BSA loaded on silica nanoparticles showed a BSA-specific immune response in the order of S1 > S2 > SBA-15. The difference in antibody titre of SBA particles was attributed to their different *in vitro* release profiles with S1 having a cumulative in vitro release of 8% compared to SBA-15 with an in vitro release of 48% after 24 hr.

Immunisation of mice with Opti-E2

To determine if HMSA can act as a useful delivery vehicle for the BVDV E2 protein, mice were immunised with the Opti-E2 nanovaccine formulation. The Group 1 mice received 50 μg Opti-E2 and 10 μg Quil A adjuvant, Group 2 mice received 20 μg Opti-E2/250 μg HMSA and the negative control group received 250 μg HMSA particles (Table 1). A higher dose of 50 μg Opti-E2 together with the Quil A adjuvant was used as a control as it was important to achieve a good immune response to Opti-E2 for the development of robust E2-specifc immunoassays within our laboratory. The Opti-E2 bound to HMSA was used only at 20 μg so as to limit the amount of nanoparticles injected to 250 μg.

The total IgG anti-Opti-E2 responses after three subcutaneous injections were determined for individual mice by Enzyme-linked Immunosorbent Assay (ELISA) using terminal bleed sera obtained two weeks after the third injection. The Opti-E2 (50ug) plus Quil A group showed excellent antibody responses at sera dilutions of 1:12800 or 10^4 titre (Fig. 7A). The mice injected with Opti-E2/HMSA nanoformulation (20 μg of Opti-E2 adsorbed to 250 μg HMSA) showed Opti-E2 specific antibody responses at 10^3 titre. There was variation between the individuals in this group with two of the mice (M1 and M2) showing higher level responses across the sera dilution series (Fig. 7B) with one mouse (M1) giving a high response at the 1:12800 dilution (Fig 7B). Control mice receiving HMSA particles showed no specific antibody response to Opti-E2 protein (Fig. 7C) and was similar to the unimmunised mice group tested (Fig. 7D).

Immune responses measured by E2-specific ELISA demonstrated development of E2-specific antibodies following two injections (data not shown) with the strongest circulating responses detected two weeks after the third injection (Fig. 7). We did observe variation in the levels of the response between individual animals receiving the nanovaccine even though we selected an inbred mouse strain for the study. The subcutaneous injections of Opti-E2 bound HMSA into mice at the tail base site did not result in localised skin redness or swelling, therefore the HMSA nanoparticles were well tolerated in mice.

Fig. 7: Immunisation of mice (n=4) with Opti-E2 bound HMSA nanoparticles. Anti-Opti-E2-specific total IgG ELISA data for the antibody response in mice immunised with: (**A**) 50 μg Opti-E2 and 10 μg Quil A, (**B**) 20 μg Opti-E2 adsorbed to 250 μg HMSA, (**C**) 250 μg HMSA particles only and (**D**) Unimmunised control group. Mice received three subcutaneous immunisations at 2 week intervals to the tail base. Preimmune (PI) sera samples were collected at the beginning of the experiment and terminal bleed sera (T) were collected two weeks following the final immunisations. Sera of individual animals (M1, M2, M3, M4) were serially diluted from 1:200 to 1:12800.

The splenocyte cell populations were used in T cell IFN-γ Enzyme-linked Immunosorbent Spot (ELISPOT) assay to determine if there was T-helper type 1 (Th1) cell-mediated immune response two weeks after the final immunisation. Fig. 8 shows the IFN-γ response of individual mice for Groups 1 to 4. The four animals in the positive Opti-E2 and Quil A group showed a very high cell-mediated immune response to Opti-E2 antigen >1400 SFU/million cell (exceeding the threshold of detection). All the mice injected with the Opti-E2 nanovaccine also showed excellent levels of cell-mediated immunity (from 800-1300 SFU/million cells). This result showed there was a strong Th1 cell response to immunisation with Opti-E2 bound HMSA. Although the response was not as high as with Opti-E2 plus Quil A this is most likely due to the lower dose of Opti-E2 (20 μg) used in the nanovaccine dose versus 50 μg Opti-E2 used in the Quil A adjuvant group. There was some IFN-γ response detected in the mice receiving HMSA particles only and the unimmunised group (Fig. 8). Presumably this background was due to the presence of the bacterially derived Opti-E2 antigen in these wells since the corresponding no antigen control wells for both of these groups had negligible SFU counts.

Previously we have conducted immunisation experiments in mice with OVA loaded amino functionalised MCM-41 type silica nanoparticles (AM-41) which gave antibody as well as cell-mediated responses.[28] However E2 loaded onto AM-41 resulted in no detectable antibody responses following three subcutaneous injections (our unpublished data). One hypothesis for this result is that adsorbed Opti-E2 may have been internalised within the AM-41 particles which have a pore size of 3.7 nm[28] and therefore was not available to the antigen presenting cells to induce an immune response. In contrast, HMSA have mesopores of 2-3 nm and Opti-E2 (predicted physical size of 12-13 nm in length and 3-4 nm in width) may bind to the external surface of HMSA, therefore remaining available for recognition as foreign antigens by antigen presenting cells.

Fig. 8: Antigen specific IFN-γ secretion by ELISPOT assay of murine splenocytes from Opti-E2 and Quil A and Opti-E2/HMSA immunised mice. Splenocytes were stimulated *in vitro* with Opti-E2 (10 ng/µl, black bars) and compared to unstimulated cells (spotted bars). Mean Spot SFU /million cells ± standard deviation for individual mice (M1 to M4) for each group are shown. The polyclonal activator, Concavalin A, was used to confirm cell viability and functionality of the assay (data not shown).

This result is very encouraging since it is often an inherent challenge in vaccine development to induce both humoral and cellular immunity. A similar finding was found using hollow mesoporous silica nanoparticles to immunise mice with *E.coli* expressed porcine circovirus type 2 (PCV2).[27] In that study a single immunisation with a dose of 100 µg PCV2/0.7 mg particles was given intramuscularly. ELISA results showed that the highest PCV2-specific antibody serum response (serum was used a 1:100 dilution) was at three weeks after the injection. Similarly T cell proliferation assays showed that the responses were maximal at 2 and 4 weeks following immunisation. Although to date there are only a few studies in which silica nanoparticles have been used to deliver proteins in animals, the biocompatibility and biodistribution of silica nanoparticles in mice has been established as they have been used more extensively for the delivery of drugs. Recently we have reviewed the biocompatibility and biodistribution of mesoporous silica nanoparticles for biomedical applications,[48] however the longer term effect of their use remains to be assessed.

Conclusion

In summary we have shown that the BVDV E2 recombinant protein adsorbed to HMSA and given via the subcutaneous route elicited both antibody and cell-mediated immune responses. *In vitro* and *in vivo* data of this study support the biocompatibility of HMSA particles. This work has demonstrated that there is potential for the development of a new generation of recombinant subunit vaccines using nanoparticle formulations which generate strong and balanced immunological responses in mammalian systems in the absence of adverse reactions.

Experimental

Nanoparticle Synthesis

Hollow mesoporous silica nanoparticles with amino groups added to the surface (HMSA) were synthesised using a modified protocol of Chen *et al.*[31] In a typical synthesis, a mixture of 60 ml absolute ethanol, 1 ml of deionised water and 3 ml 25% wt/volume ammonia solution was stirred for 30 min at 50 °C. Then 2.3 ml tetraethyl orthosilicate (TEOS) was added to the solution and the mixture was stirred for another 6 hr at 50 °C. After that the temperature of the solution was adjusted to 30 °C.A mixture of 1.5 ml TEOS, 0.7 ml octadecyltrimethoxysilane (C_{18}TMS) and 0.2 ml (3-Aminopropyl)triethoxysilane (APTES) was added to the above solution and allowed to stir for 1 hr. The resulting particles were collected via high speed centrifugation. The recovered particles were dispersed in 50 ml 0.6 M Na_2CO_3, heated to 80 °C and stirred for 2 hr. The resulting hollow silica spheres were collected via centrifugation and washed 5 times with deionised water.

Characterisation of HMSA

Nitrogen adsorption-desorption analysis was performed on a TriStar II surface area and porosity analyser (Micromeritics) at liquid nitrogen temperature (-196 °C). The particle surface area was calculated by the Brunauer–Emmet–Teller (BET) method using multiple points over the linear part of the plot (P/P0 range 0.05-0.25). Pore diameter distribution was determined by the Barrett-Joyner-Halenda (BJH) method and pore volume was estimated from the amount of nitrogen adsorbed at a relative pressure of 0.99. For transmission electron microscopy (TEM) imaging the HMSA sample (1 mg/ml) was dispersed in ethanol and sonicated using a probe (Hielscher UP100H) at 60% amplitude for 2 min at room temperature. A drop of the nanoparticle suspension was deposited on carbon film copper grids and TEM images were collected by a JEOL JEM-1010 (Tokyo, Japan) with an acceleration voltage of 100 kV. A sample (5 mg/ml suspension) was similiarly prepared for scanning electron microscopy (SEM) imaging, with the addition of coating of the sample with 5 nm platinum for SEM observation using a FEI Quanta 450 scanning electron microscope. Amino functionalisation of the nanoparticles was characterised using X-ray photoelectron spectroscopy (XPS) using AlKα radiation. Fourier transform infrared (FTIR) spectra were recorded on a Thermo Scientific NICOLET 6700 FTIR spectrometer.

In vitro cytotoxicity assay by trypan blue staining

Madin-Darby bovine kidney (MDBK) cells (ATCC CCL 22) were seeded at 80-90% confluency onto glass coverslips in a 24 well plate and allowed to adhere overnight in a 37 °C, 5% CO_2 incubator. To investigate the effect of nanoparticle concentration on the cells, a dilution range (0.5 mg/ml, 0.1 mg/ml and 0.01 mg/ml) of HMSA in Earle's Minimum Essential Media (containing 5% foetal bovine serum, Life Technologies) were prepared and gently added drop wise to the adherent cells. As a control to induce 0.5 mg/ml MCM-41 particles were used as these were known to be cytotoxic. The cells were incubated in the presence of HMSA or MCM-41 particles at 37 °C, 5% CO_2 for 20 hr. Media was carefully removed and the wells were gently washed three times with PBS (137 mM NaCl, 2.7 mM KCl, 10 mM Phosphate buffer (pH 7.2) to remove the nanoparticles. To determine cell viability 0.2% trypan blue stain (Life Technologies) was added for 2 min. Trypan blue stain was carefully removed and the wells were washed once with PBS. Cells were fixed in 4% paraformaldehyde (PFA) pH 7.4 for 15 min, and then washed three times with PBS. Coverslips were mounted with 5 µl of MOWIOL (Sigma). Cell viability was determined by imaging on a Zeiss HAL100 microscope under bright field.

Cloning, expression, purification and solubilisation of Opti-E2

An *E. coli* codon-optimised, truncated version of E2 (which lacks the membrane binding domain of native BVDV E2) was PCR amplified and cloned into the pET-SUMO bacterial expression vector with further modification to remove the SUMO expression tag, as described previously.[16] The large-scale expression, purification and

solubilisation of Opti-E2 protein was performed as described previously for E2 protein.[49]

Opti-E2 adsorption isotherm reactions

Suspensions of HMSA (10 mg/ml in 50 mM Tris (pH7.0), 0.2% Igepal CA630 in a 10 ml volume) were ultrasonicated (1 min, room temperature) using a 5 mm probe sonicator (Hielscher UP100H, Teltow, Germany) set at 80% amplitude. Adsorption reactions were performed at 25 °C in 50 mM Tris, 0.2% Igepal CA630 buffer (pH 7.0) which is the pH at which maximal binding will occur since the calculated isoelectric point of Opti-E2 is 7.25.[16] To determine the HMSA-Opti-E2 isotherm four adsorption reactions (2 ml total volume) were performed with various amount of Opti-E2 protein with a constant particle concentration (1 mg/ml). The protein:particle ratios used were 150, 100, 87.5 and 75 µg Opti-E2 protein/mg HMSA particles. The adsorption reactions were placed in a shaker (200 rpm) at 25 ^{o}C. At the time points of 4 and 22 hr a 200 µl sample of the particle-protein slurry was removed and centrifuged (16.2 *g*, 1 min). The amount of Opti-E2 protein remaining in the adsorption supernatants were visualised by gel electrophoresis and quantified using a microtitre plate format protein assay kit (Biorad DC kit, Hercules, USA) following the manufacturer's instructions.

***In vitro* desorption of Opti-E2 protein**

To determine whether there is desorption of Opti-E2 after binding to HMSA, *in vitro* desorption studies were performed. Opti-E2 loaded particles (200 µg Opti-E2/2mg HMSA) were suspended in prewarmed (37 °C) injectable saline solution (0.9% sodium chloride, 1 ml, Pfizer, Brooklyn, USA) and incubated with shaking at 37 °C for 2 hr. The sample was centrifuged (16.2 *g*, 1 min) and the supernatant collected. The procedure was repeated using 0.1 N HCl and 0.5% SLS. The desorption supernatant and particle samples were run on SDS-PAGE gels to determine if Opti-E2 had desorbed from the particles.

SDS-PAGE Electrophoresis

SDS-PAGE analysis was performed using XCell *SureLock*® Mini-Cell precast system (Invitrogen) with NuPAGE 10% BIS-Tris gels according to manufacturer instructions. Size estimations were determined against SeeBlue® Plus2 (Invitrogen) pre-stained molecular weight standards. The resolved proteins were visualised by staining in 50% methanol, 10% acetic acid, 0.25% Coomassie Blue R250 for 30 min, followed by destaining in 30% methanol, 10% acetic acid for 10 min three times.

Western hybridisation analysis of Opti-E2

Following SDS-PAGE electrophoresis the Opti-E2 protein was immediately transferred to Hybond C nitrocellulose membrane (GE Healthcare, Buckinghamshire, United Kingdom) using Invitrogen XCell II™ Blot Module Kit according to manufacturer's instructions. All antibodies were diluted in BLOTTO (PBS (Amresco), 0.1% Tween 20, 1% skim milk). E2 specific monoclonal antibodies mAb-157 and mAb-348[50] were used at 1:100 dilution, polyclonal goat anti-BVDV (VMRD, Pullman, USA) was used at 1:500 dilution, cattle sera was used at 1:250 dilution and mice sera at 1:4000 dilution. The secondary antibody anti-mouse Immunoglobulin G HRP conjugate (Chemicon, Millipore, Billerica, Massachusetts, USA) was used at 1:2,000 dilution and anti-bovine Immunoglobulin G HRP conjugate (Zymed) at 1:10,000 dilution. Detection was carried out using an ECL detection kit (GE Healthcare).

Animals

C57BL/6J mice were purchased from and housed in the Biological Resource Facility, The University of Queensland, Brisbane, Australia under specific pathogen-free conditions. Eight week old female mice were housed in HEPA-filtered cages with 4 animals per cage in an environmentally controlled area with a cycle of 12 hr of light and 12 hr of darkness. Food and water were given *ad libitum*. All procedures were approved by The University of Queensland Ethics Committee. Animals were closely monitored throughout the study and weighed every week. All the animals remained in good health for the duration of the study with no visible deleterious health effects.

Immunisation of mice

Pre-immunisation blood samples were collected by retro-orbital bleeds using heparin coated hematocrit tubes (Hirschmann Laborgeräte, Heilbronn, Germany). Pre-immunisation blood samples collected prior to the first immunisation were referred to as the preimmune (PI) samples. Opti-E2 protein adsorption to HMSA was performed within 24 hr of animal immunisation. The Opti-E2/HMSA adsorption reactions were prepared aseptically using 200 µg Opti-E2 protein and 2 mg HMSA (10 mg/ml) in sterile 50 mM Tris, 0.2% Igepal CA630 buffer (pH 7.0) in a total volume of 2 ml at 25 °C, 200 rpm for 22 hr. Quil A (2 mg/ml, Superfos Biosector, Vedback, Denmark) was resuspended in sterile injectable water (Pfizer). All doses were prepared in injectable saline (0.9%, 100 µl) and administered by subcutaneous injection at the tail base using a sterile 27 gauge needle (Terumo, Tokyo, Japan). The injection doses administered were Opti-E2 (50 µg and 10 µg Quil A), Opti-E2-HMSA (20 µg/250 µg HMSA) and 250 µg HMSA (Table 1). Three injections were administered at 2 week intervals and mice were euthanized 14 days after the final immunisation.

Table 1: Immunisation groups (n = 4) in mice study. All doses were administered by subcutaneous injection at the tail base.

Treatment Group	Group Description	Injected dose (100 µl)
1	Opti-E2	50 µg Opti-E2 +10 µg Quil A
2	Opti-E2+HMSA	20 µg Opti-E2/250 µg HMSA
3	HMSA	250 µg HMSA
4	Unimmunised Control	N/A

E2-specific ELISA

Enzyme-Linked ImmunoSorbent Assay (ELISA) for the detection of E2-specific antibodies were performed by coating microtitre plates (96 well, Nunc, Maxisorb, Roskilde, Denmark) with Opti-E2 protein solution (100 ng/well) in PBS overnight at RT. The coating solution was removed and the plates were washed once with PBS-T (PBS (1x), Tween-20 (0.1%), Sigma-Aldrich) and blocked with Bovine Serum Albumin (BSA, 5%, Sigma-Aldrich) and skim milk (5%, Fonterra, Auckland, New Zealand) in PBS (200 µl) for 1 hr with gentle shaking at RT. Plates were washed three times with PBS-T.
Mouse sera samples were diluted from 1:100 to 1:6400 in PBS and 50 µl of each dilution was added to the wells of the blocked plates followed by incubation for 2 hr at RT. The polyclonal sheep anti-

mouse IgG Horse Radish Peroxidase conjugated secondary antibody (1:1000 in PBS, Chemicon Australia, Melbourne, VIC, Australia) was added and incubated for 1 hr at RT with gentle shaking. Plates were washed three times in PBS-T. TMB substrate (100 µl, Sigma-Aldrich) was added and incubated for 15 min at room temperature. 1N HCl (100 µl) was added to wells to stop the chromogenic reactions. The plates were read at 450 nm on a Labsystems Multiskan RC plate scanner.

Isolation of murine splenocytes and interferon-γ (IFN-γ) ELISPOT assays

Spleens were aseptically removed following euthanasia and placed into 5 ml ice cold DMEM media supplemented with 10% fetal bovine serum (FBS), 20 mM Hepes (pH 7.3), 1 M sodium pyruvate, 1 M Glutamax, 100 units/ml penicillin G, 100 µg/ml streptomycin, 0.25 µg/ml Fungizone. Spleens were gently disrupted and passed through a 100 µm nylon mesh (Becton Dickinson, Franklin Lakes, NJ) using a syringe plunger. Cells were washed with 5 ml DMEM, centrifuged (800 *g*, 5 min, 4 °C) and then resuspended in 1 ml lysis buffer (0.15 M NH_4Cl, 10 mM $KHCO_3$, 0.1 mM Na_2-EDTA for 5 min at room temperature. Wash steps were repeated twice with DMEM. Cell pellets were resuspended in 2 ml DMEM and cell numbers determined by staining with 0.2% trypan blue. Cells from each mouse spleen were seeded at 1.0 - 1.5 x 10^5 cells/well in triplicate into Polyvinylidene fluoride (PVDF) ELISPOT plates precoated with monoclonal interferon-γ (IFN-γ) (Mabtech) capture antibody. Cells were incubated in complete DMEM medium at 37°C and 5% CO_2 for 40 hr in the presence or absence of Opti-E2 protein (10 µg/ml dialysed in PBS) or the polyclonal activator concavalin A (1 µg/ml, Sigma Aldrich) as a positive control. IFN-γ ELISPOT assays were performed according to the manufacturer's specifications. The ELISPOT plates were read on an ELISPOT reader (Autoimmun Diagnostika, Strassburg, Germany).

Acknowledgements

This work was funded by the Queensland Government through its Department of Employment, Economic Development and Innovation Reinvestment Fund. We thank Margaret Commins for performing the western hybridisation analysis. We thank Prof Rajiv Khanna and Dr Corey Smith for the use of the ELISPOT reader system at The Queensland Institute of Medical Research.

[a]Queensland Alliance for Agriculture and Food Innovation, The University of Queensland, St Lucia, QLD 4072, Australia.
[b]School of Chemical Engineering, The University of Adelaide, SA 5005, Australia.

† These authors contributed equally to this paper.

Corresponding author:
Associate Professor Neena Mitter
n.mitter@uq.edu.au
Phone: +61 7 3346 6513
Facsimile: + 61 7 3346 6501.

Co-corresponding author:
Professor Shizhang Qiao
s.qiao@adelaide.edu.au
Phone: +61-8-83136443
Facsimile: +61-8-83134373

Keywords: Adjuvant, BVDV, Delivery, E2, Hollow Mesoporous Silica, Vaccine.

Electronic Supplementary Information (ESI) available: Desorption studies of Opti-E2 bound HMSA.

1. H. Houe, *Vet. Microbiol.*, 1999, **64**, 89-107.
2. H. Houe, *Biologicals*, 2003, **31**, 137-143.
3. W. Q. Ma and Y. Fang, *J. Colloid Interface Sci.*, 2006, **303**, 1-8.
4. B. E. Hessman, R. W. Fulton, D. B. Sjeklocha, T. A. Murphy, J. F. Ridpath and M. E. Payton, *Am. J. Vet. Res.*, 2009, **70**, 73-85.
5. H. J. Thiel, M. S. Collett, E. A. Gould, F. X. Heinz, M. Houghton, G. Meyers, R. H. Purcell and C. M. Rice, in *Virus Taxonomy. Eighth Report on the International Committee on the Taxonomy of Viruses.*, eds. C. M. Fauquet, M. A. Mayo, J. Maniloff, U. Desselberger and L. A. Ball, Academic Press, Amsterdam2005, pp. 981-998.
6. R. O. Donis, W. Corapi and E. J. Dubovi, *J. Gen. Virol.*, 1988, **69**, 77-86.
7. M. Yu, A. R. Gould, C. J. Morrissy and H. A. Westbury, *Virus Res.*, 1994, **34**, 178-186.
8. G. Donofrio, E. Bottarelli, C. Sandro and C. F. Flammini, *Clin. Vaccine Immunol.*, 2006, **13**, 698-701.
9. C. Thomas, N. J. Young, J. Heaney, M. E. Collins and J. Brownlie, *Vaccine*, 2009, **27**, 2387-2393.
10. O. Iourin, K. Harlos, K. El Omari, W. X. Lu, J. Kadlec, M. Iqbal, C. Meier, A. Palmer, I. Jones, C. Thomas, J. Brownlie, J. M. Grimes and D. I. Stuart, *Acta Crystallogr F*, 2013, **69**, 35-38.
11. A. Pande, B. V. Carr, S. Y. C. Wong, K. Dalton, I. M. Jones, J. W. McCauley and B. Charleston, *Virus Res.*, 2005, **114**, 54-62.
12. Y. Li, J. M. Wang, R. Kanai and Y. Modis, *Proc. Natl. Acad. Sci. U. S. A.*, 2013, **110**, 6805-6810.
13. F. Ferrer, S. C. Zoth, G. Calamante and O. Taboga, *J. Virol. Methods*, 2007, **146**, 424-427.
14. M. P. Marzocca, C. Seki, S. M. Giambiagi, B. Robiolo, R. Schauer, M. J. D. Santos, E. A. Scodeller, J. L. La Torre, A. Wigdorovitz and P. R. Grigera, *J. Virol. Methods*, 2007, **144**, 49-56.
15. R. Patterson, J. Nerren, M. Kogut, P. Court, B. Villarreal-Ramos, H.-M. Seyfert, P. Dalby and D. Werling, *Developmental & Comparative Immunology*, 2012, **37**, 107-114.
16. A. S. Cavallaro, D. Mahony, K. T. Mody, T. J. Mahony and N. Mitter, in *Advances in Virus Research II*, iConcept Press2013.
17. G. Nelson, P. Marconi, O. Periolo, J. La Torre and M. A. Alvarez, *Vaccine*, 2012.
18. H. X. Sun, Y. Xie and Y. P. Ye, *Vaccine*, 2009, **27**, 1787-1796.
19. M. L. Mbow, E. De Gregorio, N. M. Valiante and R. Rappuoli, *Curr. Opin. Immunol.*, 2010, **22**, 411-416.
20. R. Schirmbeck, K. Melber, T. Mertens and J. Reimann, *J. Virol.*, 1994, **68**, 1418-1425.
21. P. Traquina, M. Morandi, M. Contorni and G. Van Nest, *J. Infect. Dis.*, 1996, **174**, 1168-1175.
22. J. M. Brewer, M. Conacher, A. Satoskar, H. Bluethmann and J. Alexander, *Eur. J. Immunol.*, 1996, **26**, 2062-2066.
23. R. K. Gupta, B. E. Rost, E. Relyveld and G. R. Siber, *Pharm. Biotechnol.*, 1995, **6**, 229-248.

24. L. P. Mercuri, L. V. Carvalho, F. A. Lima, C. Quayle, M. C. A. Fantini, G. S. Tanaka, W. H. Cabrera, M. F. D. Furtado, D. V. Tambourgi, J. D. R. Matos, M. Jaroniec and O. A. Sant'Anna, *Small*, 2006, **2**, 254-256.
25. L. V. Carvalho, C. Ruiz Rde, K. Scaramuzzi, E. B. Marengo, J. R. Matos, D. V. Tambourgi, M. C. Fantini and O. A. Sant'Anna, *Vaccine*, 2010, **28**, 7829-7836.
26. T. Y. Wang, H. T. Jiang, Q. F. Zhao, S. L. Wang, M. J. Zou and G. Cheng, *Int. J. Pharm.*, 2012, **436**, 351-358.
27. H. C. Guo, X. M. Feng, S. Q. Sun, Y. Q. Wei, D. H. Sun, X. T. Liu, Z. X. Liu, J. X. Luo and H. Yin, *Virol. J.*, 2012, **9**, 108.
28. D. Mahony, A. S. Cavallaro, F. Stahr, T. J. Mahony, S. Z. Qiao and N. Mitter, *Small*, 2013, **9**, 3138-3146.
29. Y. S. Li, J. L. Shi, Z. L. Hua, H. R. Chen, M. L. Ruan and D. S. Yan, *Nano Lett.*, 2003, **3**, 609-612.
30. Y. F. Zhu, J. L. Shi, W. H. Shen, X. P. Dong, J. W. Feng, M. L. Ruan and Y. S. Li, *Angew Chem Int Edit*, 2005, **44**, 5083-5087.
31. Y. Chen, H. Chen, L. Guo, Q. He, F. Chen, J. Zhou, J. Feng and J. Shi, *ACS Nano*, 2010, **4**, 529-539.
32. A. Salvador, M. Igartua, R. M. Hernandez and J. L. Pedraz, *J Drug Deliv*, 2011, **181646**.
33. G. Nelson, P. Marconi, O. Periolo, J. La Torre and M. a. A. Alvarez, *Vaccine*, 2012, **30**, 4499-4504.
34. E. Dietrich, H. Oudadesse, A. Lucas-Girot, Y. Le Gal, S. Jeanne and G. Cathelineau, *Appl. Surf. Sci.*, 2008, **255**, 391-395.
35. A. S. M. Chong and X. S. Zhao, *J. Phys. Chem. B*, 2003, **107**, 12650-12657.
36. K. Barquist and S. C. Larsen, *Microporous Mesoporous Mater.*, 2010, **130**, 197-202.
37. M. Fisichella, H. Dabboue, S. Bhattacharyya, M. L. Saboungi, J. P. Salvetat, T. Hevor and M. Guerin, *Toxicol. in Vitro*, 2009, **23**, 697-703.
38. M. J. K. Thomas, I. Slipper, A. Walunj, A. Jain, M. E. Favretto, P. Kallinteri and D. Douroumis, *Int. J. Pharm.*, 2010, **387**, 272-277.
39. D. M. Huang, T. H. Chung, Y. Hung, F. Lu, S. H. Wu, C. Y. Mou, M. Yao and Y. C. Chen, *Toxicol. Appl. Pharmacol.*, 2008, **231**, 208-215.
40. T. Heikkila, H. A. Santos, N. Kumar, D. Y. Murzin, J. Salonen, T. Laaksonen, L. Peltonen, J. Hirvonen and V. P. Lehto, *Eur. J. Pharm. Biopharm.*, 2010, **74**, 483-494.
41. K. Qiu, W. Feng, X. Mo and C. He, *J. Controlled Release*, 2013, **172**.
42. J. C. Duan, Y. B. Yu, Y. Li, Y. Yu, Y. B. Li, X. Q. Zhou, P. L. Huang and Z. W. Sun, *PLoS One*, 2013, **8**.
43. A. Katiyar, L. Ji, P. G. Smirniotis and N. G. Pinto, *Microporous Mesoporous Mater.*, 2005, **80**, 311-320.
44. H. H. P. Yiu, C. H. Botting, N. P. Botting and P. A. Wright, *Phys. Chem. Chem. Phys.*, 2001, **3**, 2983-2985.
45. A. Roy, A. Kucukural and Y. Zhang, *Nat. Protoc.*, 2010, **5**, 725-738.
46. Y. Zhang, *BMC Bioinformatics*, 2008, **9**.
47. K. El Omari, O. Iourin, K. Harlos, J. M. Grimes and D. I. Stuart, *Cell reports*, 2013, **3**, 30-35.
48. K. T. Mody, A. Popat, D. Mahony, A. S. Cavallaro, C. Z. Yu and N. Mitter, *Nanoscale*, 2013, **5**, 5167-5179.
49. A. S. Cavallaro, D. Mahony, M. Commins, T. J. Mahony and N. Mitter, *Microb. Cell Fact.*, 2011, **10**, 57.
50. D. Deregt, S. A. Masri, H. J. Cho and H. Bielefeldt Ohmann, *Can. J. Vet. Res.*, 1990, **54**, 343-348.